Heliyon 10 (2024) e29218

Contents lists available at ScienceDirect

Heliyon

journal homepage: www.cell.com/heliyon

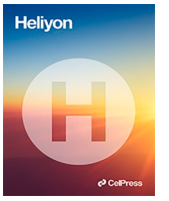

Research article

Epigenetic regulation of FOXI2 promotes clear cell renal cell carcinoma progression

Shuai Zhou [a,b], Cong Cheng [a,b], Yi xiang Liao [a,b], Li Wang [a,b], Jin min Zeng [a,b], Fang fang Zhou [a,b], Xiu qin Zhang [a,b], Tao Yang [a,b,*]

[a] Department of Urology, Jing Zhou Hospital Affiliated to Yangtze University, PR China
[b] The Second Clinical Medical College to Yangtze University, Jing Zhou City 434020, Hubei Province, PR China

ARTICLE INFO

Keywords:
FOXI2
Methylation
Renal cancer
Cell cycle arrest

ABSTRACT

In recent decades, substantial advancements in epigenetics have unveiled a profound understanding of its mechanisms in tumorigenesis and have offered promising strategies for epigenetic therapy in cancer patients. In our study, through bioinformatics analysis, we discovered a significant downregulation and hypermethylation of FOXI2 in clear cell renal cell carcinoma (ccRCC), while the expression in chromophobe cell carcinoma (chRCC) exhibited the opposite trend. Moreover, we established a strong correlation between FOXI2 expression levels and the prognosis of ccRCC. Gene enrichment analysis and cell function experiments unequivocally demonstrate that FOXI2 possesses the capability to induce cell cycle arrest and inhibit cell proliferation.

Our research findings demonstrate that the expression of FOXI2 in ccRCC is under the regulation of promoter hypermethylation. Furthermore, in vitro experiments have conclusively shown that the overexpression of FOXI2 induces cell cycle arrest and inhibits cell proliferation.

1. Introduction

Renal cell carcinoma (RCC) is one of the most common types of cancer in the urinary system, various histotypes of RCC have been defined on the basis of their histologic appearance, the most common subtype being ccRCC, papillary renal cell carcinoma (pRCC) and chRCC, representing 75–80%, 10–15% and 5% of all RCC respectively. Among these, ccRCC exhibits the highest rates of local spread, metastasis and mortality compared to pRCC especially to chRCC [1–4]. Fuhrman nuclear grade system has been the most widely used grading system, and the WHO/ISUP grading system has now been implemented in ccRCC and pRCC, while, there is no effective diagnosis biomarker used in ccRCC [5–7]. Additionally, renal cancer patients exhibit poor responses to radiation therapy and conventional chemotherapy, with surgical resection in the early stages of the tumor representing the most effective treatment option [8,9]. Therefore, there is an urgent need for a more profound understanding of the mechanisms underlying ccRCC pathogenesis, as well as improved diagnostic and therapeutic strategies.

DNA methylation plays a pivotal role as an epigenetic mechanism involved in various types of cancer, including RCC. The cancer phenotype is defined by profound changes in DNA methylation patterns and chromatin structure. Notably, the aberrant hypermethylation of gene promoters, particularly those of tumor suppressor genes, significantly contributes to tumorigenesis [10–12].

* Corresponding author. Department of Urology, Jing Zhou Hospital Affiliated to Yangtze University, PR China .
E-mail address: yt02369@yangtzeu.edu.cn (T. Yang).

https://doi.org/10.1016/j.heliyon.2024.e29218
Received 3 November 2023; Received in revised form 2 April 2024; Accepted 2 April 2024
Available online 4 April 2024

In this study, we performed comprehensive bioinformatics analyses on gene expression and methylation sequencing data obtained from ccRCC and chRCC samples within the Cancer Genome Atlas (TCGA) dataset. Our results revealed a substantial downregulation and hypermethylation of FOXI2 in ccRCC, contrasting with its expression pattern in chRCC. Notably, the expression level of FOXI2 exhibited a robust correlation with the prognosis of ccRCC patients. Lower FOXI2 expression levels were associated with a more unfavorable prognosis, paralleled by higher methylation levels. Our hypothesis suggests that the downregulation of FOXI2 may contribute to the progression of ccRCC. To substantiate this hypothesis, we conducted a series of in vitro studies aimed at elucidating the functions and mechanisms of FOXI2 in renal tumor cell proliferation and cell cycle regulation.

2. Materials and methods

2.1. Sample collection and data sources

We analyzed 24 paired samples of ccRCC tissues and adjacent normal tissues. The tissues were sequentially collected from patients who underwent radical nephrectomy between September 2021 and September 2022 at Jing Zhou Central Hospital. The utilization of samples for all experiments was conducted with the informed consent of the patients and the approval of the Ethics Committee of The Second Clinical Medical College, Yangtze University, The ethical approval number 2021-084-01. The corresponding noncancerous tissues were collected at a minimum distance of 5 cm from the tumor site, The tissue obtained from a kidney resection is immediately cut into small slices of 2 mm thickness after being detached. These slices are then packaged into four frozen storage tubes, each containing 1.5 ml of RNAwait preservation solution (Biosharp, China). After thorough mixing, the tubes are placed in a cooler box and stored in a −80 °C freezer on the same day. According to the instructions of the RNAwait preservation solution, tissues preserved in RNAwait can be stored for an extended period at −80 °C, ensuring the stability and non-degradation of RNA.

2.2. Data acquisition

Gene expression sequencing and methylation sequencing data pertaining to ccRCC and chRCC, along with the corresponding clinical data of ccRCC patients, were retrieved from The UCSC Cancer Genomics Browser (https://genome-cancer.ucsc.edu) and MEXPRESS (https://mexpress.be/) [13,14].

2.3. Cell culture, infection and transfection

All cell lines were cultured under standard conditions (37 °C, 5% CO2, humidified atmosphere) using their respective recommended media: HEK293T and ACHN in DMEM and 786-O, CaKi-1 and OS-RC-2 in RPMI-1640. All media were supplemented with 10% FBS and 2 mmol/L L-glutamine.

2.4. Plasmids and stable transfected cells establishment

The FOXI2 cDNA was amplified by PCR using KOD-Plus-Neo and then directionally cloned into the *Eco*RI and *Bam*HI sites of the lentiviral vector pCDH-CMV-MCS-copGFP-puro (System Biosciences). HEK293T cells were transfected with the lentiviral construct along with helper plasmids to generate recombinant lentivirus. Target cells were then infected with the lentivirus, followed by puromycin selection to obtain stable cell lines for further experiments. All cell lines were obtained from the National Collection of Authenticated Cell Cultures of China. The EZH2 knockout 786-O cell as well as the two shRNA interference plasmids targeting EZH2 were generously provided by Professor Chen Ke from the Department of Urology at Wuhan Tongji Hospital [15].

2.5. Quantitative real-time PCR (qRT-PCR), western blot analysis

To assess the efficiency of FOXI2 overexpression, qRT-PCR was conducted using SYBR Premix Ex TaqTM (Takara Bio, Dalian, China), following the manufacturer's guidelines. The primer sequences for quantitative detection and full-length amplification are provided in the supplement.

For Western blot analysis, the indicated cells were harvested, and proteins were extracted using NP-40 lysis buffer. Immunoblot analysis was performed according to previously described procedures by the research team led by Professor Chen [15]. Primary antibodies against P21, CDK4, CDK6 (dilution 1:1000; CST), EZH2 (dilution 1:2000; Proteintech), Beta Actin (dilution 1:2000; Proteintech), FOXI2 (dilution 1:1000; SANTA CRUZ) and tubulin (dilution 1:1000; Affinity) were used.

2.6. Cell proliferation, and flow cytometric analysis

Cell viability was assessed at 0, 12, 24, 48, and 72 h after stable transfection with the PCDH or FOXI2 overexpression plasmid in 786-O and ACHN cells using the MTS assay (CellTiter 96® AQueous Non-Radioactive Cell Proliferation Assay Promega) in accordance with the manufacturer's instructions. Each MTS assay was conducted with five replications.

To investigate the impact of FOXI2 overexpression on cell cycle progression, cells were transfected with either a control PCDH plasmid or a FOXI2 overexpression plasmid. Following transfection, 2 x 10^5 cells per well were seeded in 6-well plates. To synchronize the cell cycle, they were then subjected to serum starvation for 24 h in serum-free medium. After starvation, fresh growth medium was

added for 48 h. Subsequently, cells were harvested for cell cycle analysis using propidium iodide (PI) staining with the BD Cycletest Plus DNA Reagent Kit (125 μg/mL, BD Biosciences, MA, USA). Flow cytometry was performed on a Beckman CytoFLEX system (USA) to quantify the cell cycle distribution of PCDH and FOXI2-overexpressing cells. This analysis focused on determining and comparing the percentages of cells in the G0/G1, S, and G2/M phases of the cell cycle between the two groups.

2.7. Methylation status analysis and demethylation assay

Quantitative methylation analysis of the FOXI2 promoter region was conducted using the Sequenom MassARRAY platform (oebiotech, Shanghai, China), following the manufacturer's protocol. Detailed information regarding primers and detecting sequences is provided in the supplementary materials. To ascertain whether FOXI2 expression can be induced following demethylation, four RCC cell lines, namely CAKI-1, ACHN, 786-O, and OS-RC-2, were treated with varying concentrations of 5-aza-2′-deoxycytidine (5-aza-dC).

2.8. Statistical analysis

Statistical analyses were conducted using R version 3.30. The significance of differences between groups was assessed using either the student's t-test or the $\chi 2$ test, as appropriate. Univariate and multivariate analyses of overall survival (OS) and disease-free survival (DFS), considering FOXI2 expression, methylation levels at specific FOXI2 sites, and clinicopathological factors, were performed using the R package "survival" [16].

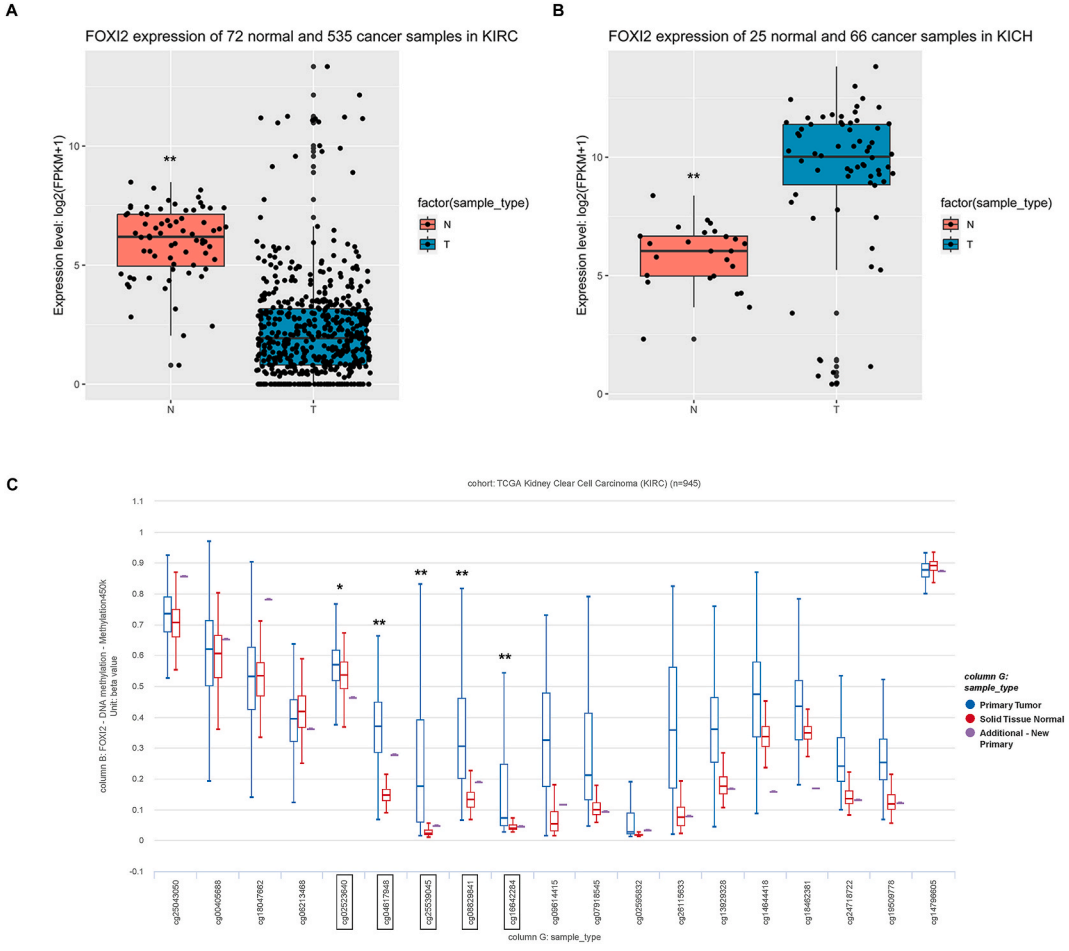

Fig. 1. FOXI2 was downregulated and hypermethylated in ccRCC while opposite in chRCC. (A, B) The expression of FOXI2 in ccRCC, chRCC tissues and their normal counterparts from TCGA Data Portal, ** , $P < 0.001$. (C) Detailed methylation profile of FOXI2 in tumor and normal tissues in ccRCC, the black boxes highlight five methylation test probes upstream of the gene.

3. Results

3.1. FOXI2 downregulation and hypermethylation in ccRCC contrasts with chRCC

The expression and methylation profiles of FOXI2 in ccRCC and chRCC were extracted from The UCSC Cancer Genomics Browser and MEXPRESS within The Cancer Genome Atlas (TCGA) dataset. Remarkably, FOXI2 exhibited significant downregulation and pronounced hypermethylation in ccRCC, whereas the opposite trend was observed in chRCC (Fig. 1A–C and Fig. 2A).

Due to the unavailability of matched normal tissues in the HumanMethylation 450 KICH dataset, we couldn't directly compare methylation levels between tumor and normal tissues in chRCC. Nevertheless, an observable trend of relatively higher methylation

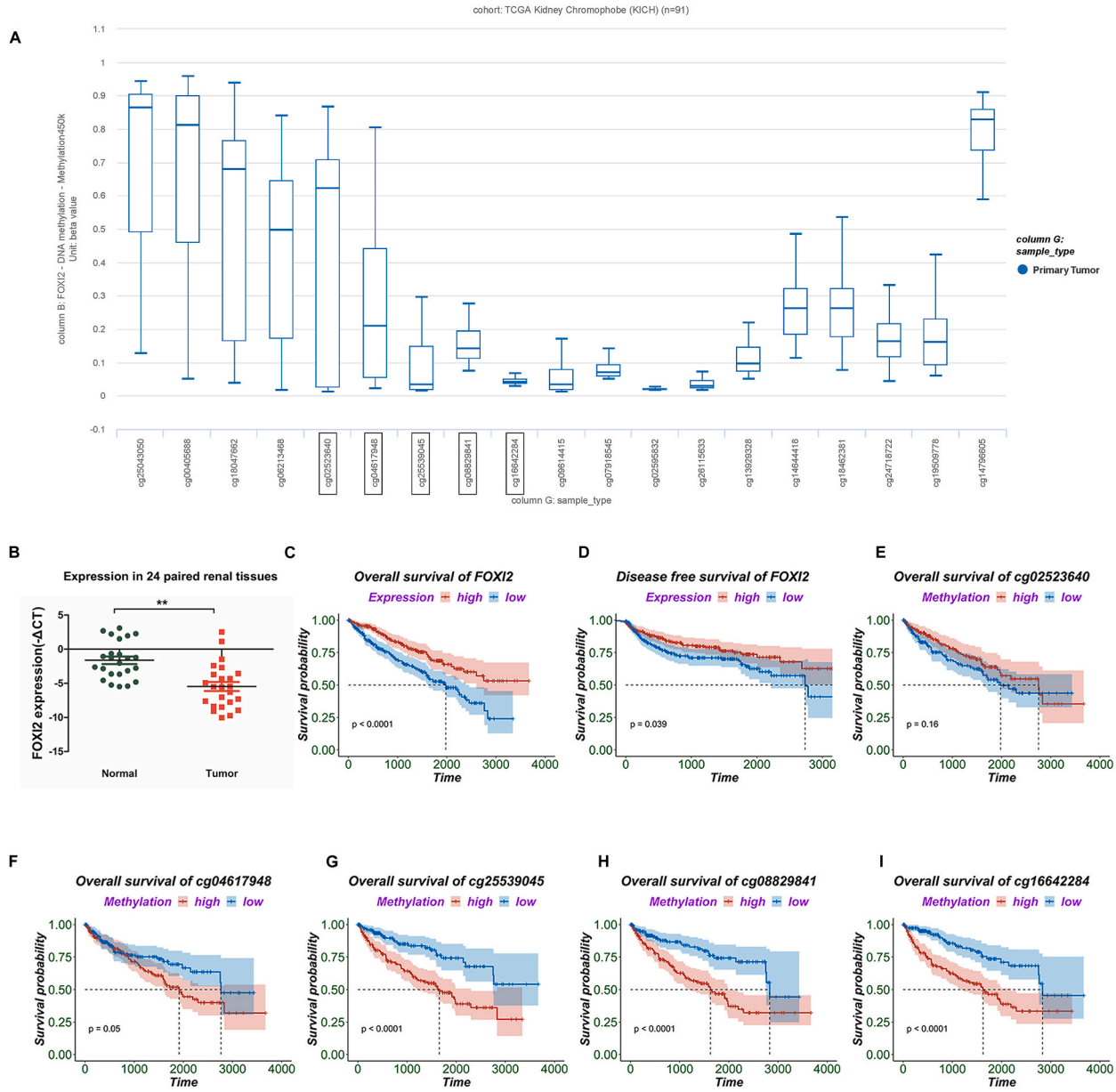

Fig. 2. The expression and methylation profile of FOXI2 are correlated with clinical progress in ccRCC. (A)Detailed methylation profile of FOXI2 in tumor tissues in chRCC from TCGA, the black boxes highlight five methylation test probes upstream of the gene. (B) Relative expression of FOXI2 in 24 pairs of ccRCC tumor tissues and their normal counterparts, relative gene expression was determined using the comparative -delta CT method (−ΔCT, FOXI2 minus GAPDH) , **, P < 0.001. (C, D) Kaplan–Meier curves depicting overall survival and disease-free survival of ccRCC patients stratified by FOXI2 expression levels in TCGA. (E, F, G, H) Kaplan–Meier survival analysis of overall survival according to the represented methylation state in ccRCC from TCGA.

levels in tumor tissues of ccRCC patients compared to chRCC patients can be discerned from Fig. 1C and 2A.

Subsequently, we performed RT-qPCR to evaluate FOXI2 expression in 24 paired ccRCC tissues and their corresponding noncancerous tissues. The results unequivocally revealed decreased FOXI2 mRNA levels in the tumor samples when compared to the noncancerous tissues (Fig. 2B, $P < 0.001$).

3.2. Association of FOXI2 expression and methylation with clinical parameters in ccRCC

We obtained FOXI2 expression and methylation data, along with corresponding clinical information from ccRCC patients through The UCSC Cancer Genomics Browser. FOXI2 expression and methylation levels at several putative promoter region sites (the probes highlighted in black boxes in Fig. 1C and 2A) were divided into low-expression groups and high-expression based on their respective median values. Kaplan–Meier analysis and the log-rank test were utilized to evaluate the impact of FOXI2 expression on Overall Survival (OS) and Disease-Free Survival (DFS) in ccRCC patients. Additionally, we investigated the influence of specific methylation levels on OS in ccRCC patients. The results revealed that patients with lower FOXI2 expression experienced reduced OS and DFS

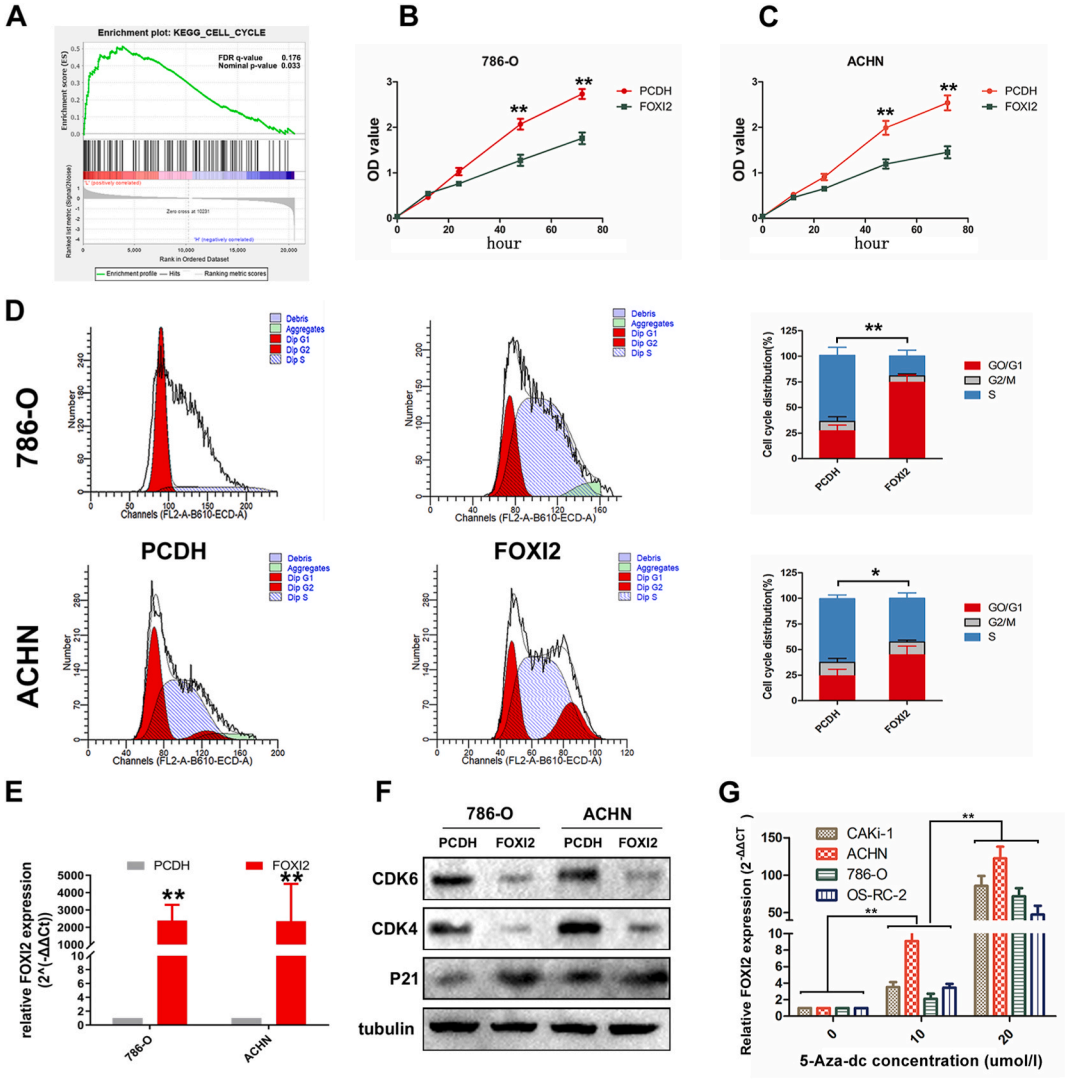

Fig. 3. Overexpression of FOXI2 inhibits cell proliferation, induces cell cycle arrest in vitro (A) GSEA of KEGG_CELL_CYCLE SIGNALIN PATYWAY in 50 samples of the highest FOXI2 expression versus 50 samples with the lowest FOXI2 expression. (B, C) MTS assays revealed cell growth curves of indicated cells. **, $P < 0.001$. (D) Flow cytometric analysis showed that FOXI2 overexpression increased the number of cells in the G0/G1 phase and reduced the number of cells in the S phase, results were the mean ± SEM from three independent experiments, $P < 0.05$. (E) The efficiency of FOXI2 overexpression plasmid in renal cancer cell lines 786-O and ACHN , relative gene expression was determined using the comparative delta-delta CT method (2^(-ΔΔCt)) , ** , $P < 0.001$. (F) The levels of cell cycle-related proteins were tested by Western blot. The original blots can be found in the attached file Fig. 3 F. (G) RT-qPCR demonstrated FOXI2 expression in four renal cancer cell lines after treatment with different concentrations of 5-aza-2-deoxycytidine for 48 h, ** , $P < 0.001$.

compared to those with higher FOXI2 expression (Fig. 2C and D). Furthermore, patients with higher methylation levels at several putative promoter region sites of FOXI2 exhibited a worse prognosis (Fig. 2 F, G, H, I).

Furthermore, we found that FOXI2 expression in ccRCC was correlated with clinical parameters, including histologic grade, pathologic stage, as well as lymph node status. Lower FOXI2 expression was associated with a higher histologic grade, advanced pathologic stage, and a higher rate of lymph node positivity. Detailed data are not presented here.

3.3. *Overexpression of FOXI2 inhibits cell proliferation and induces cell cycle arrest in vitro*

To further investigate the potential function of FOXI2 in ccRCC, we utilized Gene Set Enrichment Analysis (GSEA). We analyzed the gene expression data from 50 samples with the lowest FOXI2 expression and 50 samples with the highest FOXI2 expression. The GSEA results revealed significant enrichment of gene sets associated with the cell cycle pathway in samples with low FOXI2 expression. Moreover, decreased FOXI2 expression was associated with the upregulation of genes involved in the cell cycle, suggesting a pivotal role for FOXI2 in cell cycle progression (Fig. 3A). We conducted MTS assays, which revealed that FOXI2 overexpression (Fig. 3E) resulted in decreased proliferation of 786-O and ACHN cells (Fig. 3B and C). Flow cytometric analysis demonstrated that FOXI2 overexpression increased the number of cells in the G0/G1 phase and decreased the number of cells in the S phase (Fig. 3D).

To further elucidate the molecular mechanisms underlying FOXI2-mediated proliferation, we assessed several proteins involved in cell cycle progression. As illustrated in Fig. 3F, FOXI2 overexpression resulted in the downregulation of CDK6 and CDK4, while inducing the upregulation of p21. These findings collectively underscore the role of FOXI2 in regulating the cell cycle in ccRCC, with FOXI2 overexpression promoting cell cycle arrest in 786-O and ACHN cells.

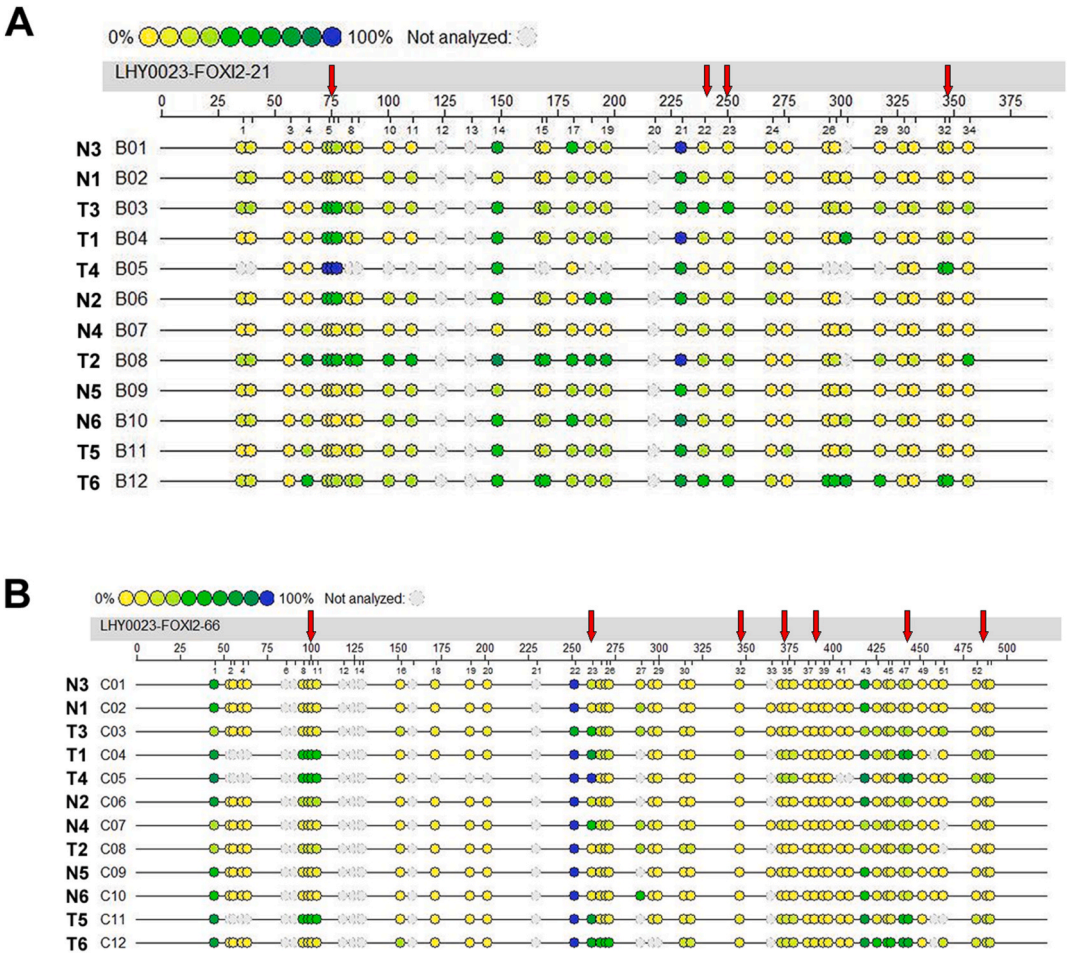

Fig. 4. Hypermethylation in CpG sites of FOXI2 in six paired ccRCC tissues (A, B) methylation state in FOXI2 promoter determined by Sequenom MassARRAY analysis in six paired ccRCC and adjacent normal tissues. Red arrows show profile of several methylation of CpG sites in the FOIX2 promoter region, with significant differences between tumor and normal tissues, $p < 0.05$. (For interpretation of the references to color in this figure legend, the reader is referred to the Web version of this article.)

3.4. Methylation of FOXI2 contributes to reduced expression in ccRCC

We also conducted a restoration experiment for FOXI2 expression using 5-aza-dC treatment. Cells were cultured with or without 10–20 μmol/L of 5-aza-dC for 48 h. The expression of FOXI2 before and after 5-aza-dC treatment was determined via RT-qPCR. Our RT-qPCR analysis demonstrated a progressive increase in FOXI2 transcript abundance following 5-aza-dC treatment (Fig. 3G).

To investigate whether promoter hypermethylation contributes to the reduced expression of FOXI2 in ccRCC, we quantitatively examined the promoter methylation status of FOXI2 using the Sequenom MassARRAY platform. CpG islands within the putative FOXI2 promoter were identified through the Methprimer database. Compared to normal tissues, the MassARRAY assay showed higher methylation levels at several tested sites and a higher average methylation level within the promoter region in six ccRCC tumor tissues (Fig. 4A and B, with red arrows indicating significantly different methylation levels at CpG sites between the N and T groups, $p < 0.05$). Specific sequencing results are provided in the attachment.

3.5. Negative correlation between EZH2 and FOXI2 expression in ccRCC: Implications for FOXI2 epigenetic silencing

Through an analysis of FOXI2 and EZH2 expression in ccRCC and chRCC within the TCGA dataset, we found that FOXI2 and EZH2 expression were negatively correlated in ccRCC. ($p < 0.001$), while no such correlation was observed in chRCC (Fig. 5B and C). To delve deeper into the epigenetic regulation of FOXI2, we explored the UCSC Genome Browser, focusing on the methylation status of FOXI2 and its interaction with the transcription factor EZH2. As illustrated in Fig. 5A, the promoter region of FOXI2 contains abundant CpG islands, and H3K27Me3 marks were identified in several cell lines, indicative of epigenetic silencing. Furthermore, the ENCODE Transcription Factor Binding tracks indicated a robust binding affinity between EZH2 and the FOXI2 promoter region in A673, GM23338, and hepatocyte cells.

To experimentally verify the role of EZH2 in FOXI2 expression, we conducted RT-PCR in EZH2 knockout 786-O cells and performed Western blot analysis of EZH2 and FOXI2 expression after EZH2 interference in ACHN and 786-O cell lines. Remarkably, we observed a notable upregulation of FOXI2 in EZH2 knockout 786-O cells compared to normal 786-O cells (Fig. 5D). Furthermore, the expression of

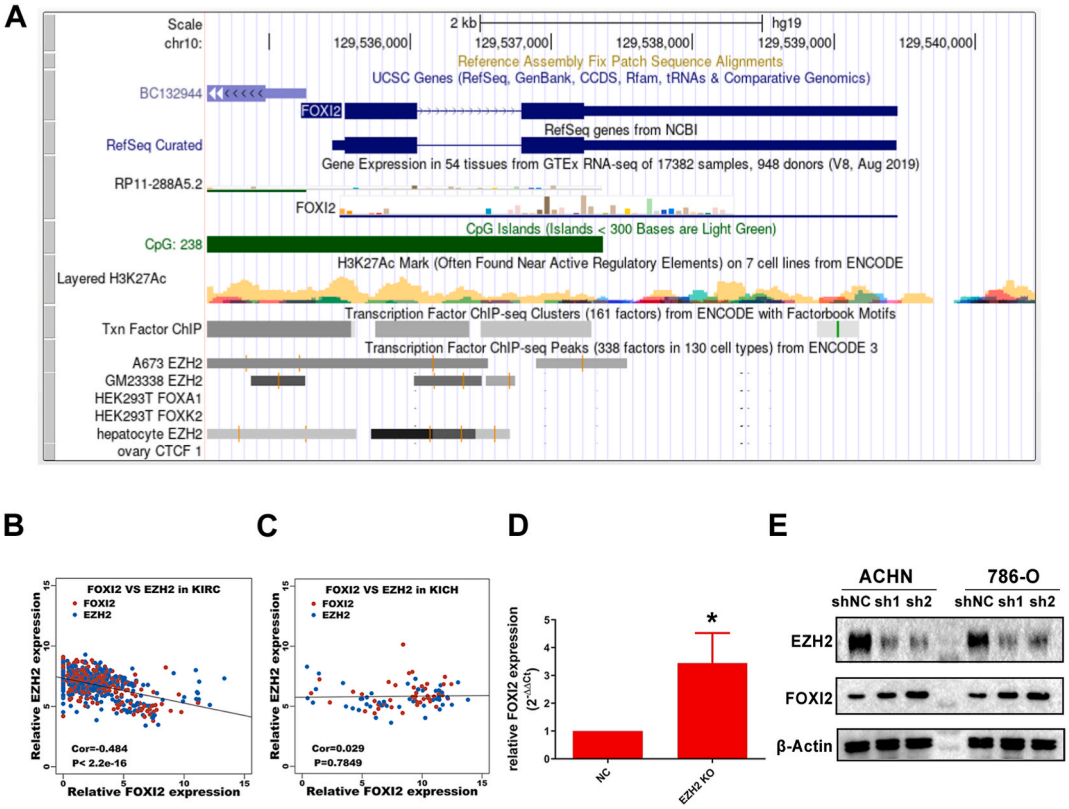

Fig. 5. The relation between the expression of FOXI2 and EZH2 in ccRCC and chRCC. And the potential effect of EZH2 on FOXI2. (A)The custom UCSC genome browser tracks showing location of FOXI2 gene, CpG islands (CpG:238), H3k27Me3 marks in several cell lines (middle colored part, scale 1 to 10) and binding capability with EZH2 in A673, GM23338 and hepatocyte cells in the FOXI2 promoter region. (B, C) The relationship between the expression of FOXI2 and EZH2 in ccRCC and chRCC in TCGA. (D) Relative expression of FOXI2 was measured by RT-qPCR in 786-O cells after EZH2 knock out *, $P < 0.05$. (E) Western blot was performed to detect the expression of EZH2 and FOXI2 in 786-O and ACHN cell lines stably transfected with shNC and shEZH2 interference plasmids, the original blots can be found in the attached file Fig. 5 E.

FOXI2 was significantly increased in ACHN and 786-O cell lines after EZH2 interference (Fig. 5E).

4. Discussion

Aberrant promoter hypermethylation, particularly affecting tumor suppressor genes, represents a prevalent mechanism for transcriptional silencing in cancer, playing a pivotal role in various malignant diseases [17–19]. Over the past two decades, extensive research has identified numerous tumor suppressor genes such as APC, APAF1, CDKN2A, and pivotal signaling pathways including the WNT–β-catenin and SLIT2–ROBO1 pathways, all of which have been found to be dysregulated or silenced through epigenetic mechanisms, primarily via the methylation of promoter CpG islands in renal cancer [20–23]. Moreover, a comprehensive molecular characterization of over 500 ccRCC samples and 161 pRCC in TCGA revealed that the overall frequency of promoter DNA hypermethylation in these tumors increases with higher stage and grade [24,25].

Our investigation into the gene and methylation profiles of two types of kidney cancer, ccRCC and chRCC, which exhibit distinct prognoses, revealed striking differences in FOXI2 expression and methylation status. FOXI2 was significantly downregulated and extensively hypermethylated in ccRCC, whereas its expression in chromophobe cell carcinoma exhibited an opposite pattern, marked by relatively lower methylation rates at corresponding CpG sites. Furthermore, lower FOXI2 expression was correlated with worse overall survival, disease-free survival, and higher stage and grade in ccRCC. Notably, the methylation levels at several CpG sites within the putative promoter region of FOXI2 displayed an inverse correlation with disease prognosis (Fig. 2F, G, H, I). These intriguing findings prompted us to investigate the potential role of FOXI2 in ccRCC, as well as the mechanisms underlying its regulation. FOXI2 is a member of the Forkhead box (Fox) protein superfamily, a group of proteins known to function as either tumor suppressors or oncogenes [26–28]. Remarkably, prior to this study, FOXI2 had not been subjected to functional investigations in neoplastic diseases, particularly in renal cell carcinoma.

In this study, we initially investigated the expression of FOXI2 in 24 paired ccRCC tissues and their corresponding adjacent normal tissues through RT-qPCR and the result is consistent with the expression profiles observed in TCGA data. Subsequently, we conducted fundamental functional studies within ccRCC cells. Remarkably, we found that FOXI2 overexpression possessed the capability to inhibit cell growth and induce cell cycle arrest in both 786-O cells and ACHN cells. Furthermore, our Western blot analyses provided further evidence of FOXI2's tumor-suppressive role by demonstrating its downregulation of CDK6 and CDK4 expression while upregulating p21 expression. These results underscore the pivotal function of FOXI2 in inhibiting cell proliferation and inducing cell cycle arrest.

In addition to functional experiments, we utilized Sequenom MassARRAY to analyze the methylation status of FOXI2 promoter region in six paired ccRCC tissues. Notably, the average methylation level of the promoter region and methylation levels at several CpG units (highlighted by red arrows) were significantly different in tumor and paired normal tissues, with an overall higher methylation level in the tumor tissues (Fig. 4A and B). Interestingly, treatment of four ccRCC cell lines with 10–20 μmol/L of 5-aza-dC for 48 h resulted in a substantial increase in FOXI2 expression (Fig. 3G). This observation supports the hypothesis of epigenetic silencing of FOXI2 through methylation of promoter CpG islands and encourages further exploration of the potential mechanisms underlying FOXI2 methylation.

To delve deeper into this mechanism, we examined the relationship between FOXI2 expression and EZH2, a histone methyltransferase. We observed an inverse correlation between FOXI2 and EZH2 expression in ccRCC, but not in chRCC (Fig. 5B and C). We also explored the UCSC genome browser to investigate the potential role of histone modifying factors, such as EZH2, in mediating H3K27 trimethylation (H3K27me3) and their binding to the FOXI2 promoter. The promoter region of FOXI2 was found to contain abundant CpG islands, and H3K27me3 marks were detected in several cell lines. Moreover, strong binding capability with EZH2 was observed in the FOXI2 promoter region in A673, GM23338, and hepatocyte cells, according to ENCODE Transcription Factor Binding tracks (Fig. 5A). To further corroborate our findings, we examined FOXI2 expression by RT-PCR in EZH2 knockout 786-O cells, which exhibit weakened histone methyltransferase activity [15]. Interestingly, we observed relatively increased FOXI2 expression in EZH2 knockout 786-O cells compared to normal 786-O cells (Fig. 5D). We further performed Western blot analysis to analyze EZH2 and FOXI2 expression following EZH2 knockdown in both 786-O and ACHN cell lines. Similarly, our results revealed that FOXI2 expression was significantly upregulated in both cell lines after EZH2 interference (Fig. 5E). This finding lends support to the hypothesis that EZH2 may be involved in the methylation process of FOXI2. However, further experiments, such as RNA immunoprecipitation (RIP) and Chromatin Immunoprecipitation Assay, are necessary to confirm this assumption.

5. Conclusions

In summary, our research highlights the differential expression and methylation profiles of FOXI2 in ccRCC and chRCC, which are correlated with clinical parameters and patient survival in ccRCC. Our study provides the first functional annotation of FOXI2 as a tumor suppressor gene in ccRCC, demonstrating its ability to inhibit cell growth and induce cell cycle arrest in vitro by regulating cell cycle-related proteins such as CDK6, CDK4, and p21. Additionally, our findings suggest that EZH2 may play an important role in the epigenetic silencing of FOXI2 in ccRCC. Therefore, strategies aimed at either specifically reprogramming the FOXI2 promoter or targeting FOXI2-dependent downstream pathways may represent potent therapeutic approaches that warrant further exploration.

Ethics approval

This study was performed in line with the principles of the Declaration of Helsinki. Approval was granted by the Ethics Committee

of Jing Zhou Hospital Affiliated to Yangtze University (No.2021-084-01).

Consent to participate

Informed consent was obtained from all individual participants included in the study.

Data availability statement

The datasets analyzed in this study were publicly available from the UCSC Cancer Genomics Browser (https://genome-cancer.ucsc.edu) and MEXPRESS (https://mexpress.be/), as well as supplementary material.

CRediT authorship contribution statement

Shuai Zhou: Writing – original draft, Visualization, Investigation, Data curation. **Cong Cheng:** Writing – original draft, Investigation, Formal analysis. **Yi xiang Liao:** Supervision, Resources, Funding acquisition. **Li Wang:** Data curation, Conceptualization. **Jin min Zeng:** Data curation, Conceptualization. **Fang fang Zhou:** Data curation, Conceptualization. **Xiu qin Zhang:** Data curation, Conceptualization. **Tao Yang:** Writing – review & editing, Supervision, Funding acquisition.

Declaration of competing interest

The author(s) declare(s) that there is no conflict of interest regarding the publication of this manuscript. We declare that we have no financial or non-financial interests that could be perceived as influencing the research conducted or the results presented in this paper.

Acknowledgments

We thank Professor Chen Ke for providing the EZH2 knockout 786-O cell as well as the two shRNA interference plasmids targeting EZH2 [15]. This work was supported by the National Natural Science Foundation of China (NO. 81802562), the Jing Zhou 2020 Natural Science Research Program (2020CB21-14), the scientific research project of Hubei Provincial Health and Family Planning Commission (WJ2018H208).

Appendix A. Supplementary data

Supplementary data to this article can be found online at https://doi.org/10.1016/j.heliyon.2024.e29218.

References

[1] H. Moch, A.L. Cubilla, P.A. Humphrey, et al., The 2016 WHO Classification of tumours of the urinary system and male genital organs-Part A: renal, penile, and testicular tumours, Eur. Urol. 70 (2016) 93–105, https://doi.org/10.1016/j.eururo.2016.02.029.
[2] J. Casuscelli, N. Weinhold, G. Gundem, et al., Genomic landscape and evolution of metastatic chromophobe renal cell carcinoma, J. Transl. Med. 2 (2017), https://doi.org/10.1186/s12967-017-1248-y10.1172/jci.insight.92688.
[3] K.A. Keegan, C.W. Schupp, K. Chamie, et al., Histopathology of surgically treated renal cell carcinoma: survival differences by subtype and stage, J. Urol. 188 (2012) 391–397, https://doi.org/10.1016/j.juro.2012.04.006.
[4] J.J. Hsieh, M.P. Purdue, S. Signoretti, et al., Renal cell carcinoma, Nat. Rev. Dis. Prim. 3 (2017) 17009, https://doi.org/10.1038/nrdp.2017.9.
[5] B. Delahunt, J.R. Srigley, R. Montironi, et al., Advances in renal neoplasia: recommendations from the 2012 international society of urological pathology consensus conference, Urology 83 (2014) 969–974, https://doi.org/10.1016/j.urology.2014.02.004.
[6] J.R. Srigley, B. Delahunt, J.N. Eble, et al., The international society of urological pathology (ISUP) vancouver classification of renal neoplasia, Am. J. Surg. Pathol. 37 (2013) 1469–1489, https://doi.org/10.1097/PAS.0b013e318299f2d1.
[7] S.A. Fuhrman, L.C. Lasky, C. Limas, Prognostic significance of morphologic parameters in renal cell carcinoma, Am. J. Surg. Pathol. 6 (1982) 655–663, https://doi.org/10.1097/00000478-198210000-00007.
[8] W.M. Linehan, Genetic basis of kidney cancer: role of genomics for the development of disease-based therapeutics, Genome Res. 22 (2012) 2089–2100, https://doi.org/10.1101/gr.131110.111.
[9] U. Capitanio, F. Montorsi, Renal cancer. Lancet (London, England) 387 (2016) 894–906, https://doi.org/10.1016/s0140-6736(15)00046-x.
[10] Y. Pan, G. Liu, F. Zhou, et al., DNA methylation profiles in cancer diagnosis and therapeutics, Clin. Exp. Med. 18 (2018) 1–14, https://doi.org/10.1007/s10238-017-0467-0.
[11] M.R. Morris, F. Latif, The epigenetic landscape of renal cancer. Nature reviews, Nephrology 13 (2017) 47–60, https://doi.org/10.1038/nrneph.2016.168.
[12] N. Ahuja, A.R. Sharma, S.B. Baylin, Epigenetic therapeutics: a new weapon in the war against cancer, Annu. Rev. Med. 67 (2016) 73–89, https://doi.org/10.1146/annurev-med-111314-035900.
[13] A. Koch, T. De Meyer, J. Jeschke, et al., MEXPRESS: visualizing expression, DNA methylation and clinical TCGA data, BMC Genom. 16 (2015) 636, https://doi.org/10.1186/s12864-015-1847-z.
[14] M. Goldman, B. Craft, T. Swatloski, et al., The UCSC cancer genomics browser: update 2015, Nucleic acids research 43 (2015) D812–D817, https://doi.org/10.1093/nar/gku1073.
[15] K. Chen, H. Xiao, J. Zeng, et al., Alternative splicing of EZH2 pre-mRNA by SF3B3 contributes to the tumorigenic potential of renal cancer, Clin. Cancer Res. : an official journal of the American Association for Cancer Research 23 (2017) 3428–3441, https://doi.org/10.1158/1078-0432.Ccr-16-2020.
[16] T. Therneau, A package for survival analysis in R_, R package version 3 (2020) 1–12. https://CRAN.R-project.org/package=survival.

[17] A.O. Chan, R.R. Broaddus, P.S. Houlihan, et al., CpG island methylation in aberrant crypt foci of the colorectum, Am. J. Pathol. 160 (2002) 1823–1830, https://doi.org/10.1016/s0002-9440(10)61128-5.
[18] I. Keshet, Y. Schlesinger, S. Farkash, et al., Evidence for an instructive mechanism of de novo methylation in cancer cells, Nat. Genet. 38 (2006) 149–153, https://doi.org/10.1038/ng1719.
[19] L. Di Croce, V.A. Raker, M. Corsaro, et al., Methyltransferase recruitment and DNA hypermethylation of target promoters by an oncogenic transcription factor, Science (New York, N.Y.) 295 (2002) 1079–1082, https://doi.org/10.1126/science.1065173.
[20] N. Ohtani-Fujita, T. Fujita, A. Aoike, et al., CpG methylation inactivates the promoter activity of the human retinoblastoma tumor-suppressor gene, Oncogene 8 (1993) 1063–1067.
[21] M.L. Freedman, M.R. Morris, F. Latif, The epigenetic landscape of renal cancer, Nature medicine 13 (2017) 47–60, 10.1038/s41591-020-0933-110.1038/nrneph.2016.168.
[22] F. Christoph, C. Kempkensteffen, S. Weikert, et al., Methylation of tumour suppressor genes APAF-1 and DAPK-1 and in vitro effects of demethylating agents in bladder and kidney cancer, British journal of cancer 95 (2006) 1701–1707, https://doi.org/10.1038/sj.bjc.6603482.
[23] E. Dulaimi, I. Ibanez de Caceres, R.G. Uzzo, et al., Promoter hypermethylation profile of kidney cancer, Clin. Cancer Res. : an official journal of the American Association for Cancer Research 10 (2004) 3972–3979, https://doi.org/10.1158/1078-0432.ccr-04-0175.
[24] Comprehensive molecular characterization of clear cell renal cell carcinoma, Nature 499 (2013) 43–49, https://doi.org/10.1038/nature12222.
[25] W.M. Linehan, P.T. Spellman, C.J. Ricketts, et al., Comprehensive molecular characterization of papillary renal-cell carcinoma, N. Engl. J. Med. 374 (2016) 135–145, https://doi.org/10.1056/NEJMoa1505917.
[26] D. Ni, X. Ma, H.Z. Li, et al., Downregulation of FOXO3a promotes tumor metastasis and is associated with metastasis-free survival of patients with clear cell renal cell carcinoma, Clin. Cancer Res. : an official journal of the American Association for Cancer Research 20 (2014) 1779–1790, https://doi.org/10.1158/1078-0432.ccr-13-1687.
[27] S.S. Myatt, E.W. Lam, The emerging roles of forkhead box (Fox) proteins in cancer, Nat. Rev. Cancer 7 (2007) 847–859, https://doi.org/10.1038/nrc2223.
[28] Y. Shibui, K. Kohashi, A. Tamaki, et al., The forkhead box M1 (FOXM1) expression and antitumor effect of FOXM1 inhibition in malignant rhabdoid tumor, Jouranl of cancer research and clinical oncology 147 (2021) 1499–1518, https://doi.org/10.1007/s00432-020-03438-w.